THE ROLE OF ANTIMONY IN TAILORING OPTICAL PROPERTIES OF SPRAY PYROLYSIS SYNTHESIZED PbSe/Sb THIN FILMS FOR SOLAR DEVICE OPTIMIZATION

[1]Ishiwu S.M.U., *[2]Nworie Ikechukwu C., [1, 2]Agbo P.E., [2]O.C. Nwuzor, [1]C.A. Elekwa, [2]P.B. Otah and [3]Mbamara Chinonso

[1]Department of Industrial Physics, Ebonyi State University Abakiliki, Nigeria
[2]Department of Medical and Industrial Physics, David Umahi Federal University of Health Sciences, Uburu, Nigeria
[3]Department of Industrial Physics, University of Agriculture and Environmental Science, Umuagwo, Imo State, Nigeria

*Corresponding Author Email Address:*nworieikechukwuc@*gmail.com*

ABSTRACT
In this study, we employed the Spray Pyrolysis Technique to grow thin solid films of both Antimony-doped and undoped PbSe/Sb on glass substrates. The film growth process relied on the decomposition of lead chloride ($PbCl_2$) and Antimony chloride in the presence of Sodium selenosulphide (Na_2SeSo_3). Ethylene diamine tetra acetic acid (EDTA) was utilized as a complexing agent and pH stabilizer. The determination of the films' band gaps was conducted through absorbance and transmittance measurements using a Unico-UV-2102 PC spectrophotometer, employing normal incident light in the wavelength range of 200-1500 nm. Upon annealing, thin films of undoped PbSe exhibited a higher initial absorbance of 0.70, which decreased with annealing, along with a reduced extinction coefficient from 70 to 65. Conversely, undoped PbSe displayed the highest optical conductivity, peaking at 80.4 Mmho's at λ = 340 nm, closely followed by annealed undoped PbSe. Antimony-doped PbSe films exhibited higher reflectance, transmittance, refractive index, and real dielectric constant compared to undoped PbSe. However, they had a narrower optical band gap range of 2.2 eV, which further decreased to 2.0 eV upon annealing. Notably, doping lead selenide with antimony expanded the potential applications of the films.

Keywords: Spray Pyrolysis, Bandgap, Antimony, Lead Selenide, Glass Substrates.

INTRODUCTION
In the pursuit of advancing solar energy technologies, the focus on optimizing the optical properties of thin films is paramount. Thin films, with their characteristic thickness of approximately 1μm, play a crucial role in solar device applications (Elsheikh *et al.,* 2019). Thin films, whether derived through controlled condensation of atomic, molecular, or ionic species, either by physical processes or chemical reactions on a substrate, offer a versatile platform for solar device fabrication (Eslamian, 2017). The integration of antimony into lead selenide thin films is a deliberate exploration aimed at tailoring their optical characteristics for enhanced performance in solar applications.
In a typical semiconductor, the distribution of electrons across energy levels forms filled bands, separated by a forbidden energy gap (Xia *et al.,* 2020, Akbari-Moghanjoughi, 2021). This band gap, the energy required for electrons to transition from the valence band to the conduction band (Nworie *et al.,* 2023, Endres *et al.,* 2016, Nishikawa *et al.,* 2017), is a critical determinant of the semiconductor's optical properties (Hernandez-Calderon, 2018). Depending on the intended application, a semiconductor material may require adjustments in its band gap. In cases where a precise band gap tailored for a specific application is unavailable, innovative approaches involve combining pairs of elements, neither of which necessarily needs to be a semiconductor. This has led to the development of a multitude of hybrid semiconductor materials, often referred to as militancy semiconductors (Saunders, 2020, Nelson, 2000).

Extensive research has been dedicated to thin films of lead selenide, exploring their diverse applications in optoelectronic and microelectronic devices, as well as their role in quantum engineering. Lead selenide has undergone intentional doping with various elements, including silver (Bera *et al.,* 2022), copper (Gayner *et al.,* 2016), indium (Zhang *et al.,* 2012, Ashraf *et al.,* 2017), and zinc (Ashraf *et al.,* 2016). Leveraging its extinction coefficient, optical conductivity, and other optical properties, PbSe has proven valuable in applications such as optical window coatings (Lifshitz *et al.,* 2006). To further enhance essential properties like reflectance, transmittance, refractive index, dielectric constant, and to achieve a smaller band gap for improved performance, the utilization of doping and annealing processes has been prompted. This strategic approach aims to fine-tune the optical characteristics of lead selenide thin films, opening avenues for advancements in a range of technological applications.

The introduction of antimony into lead selenide thin films through the spray pyrolysis technique presents an avenue to modulate and enhance their optical properties. The choice of antimony as a dopant is strategic, with the aim of influencing parameters such as absorption spectra and bandgap to optimize sunlight absorption—a pivotal factor in solar energy conversion (Lewis, 2016). In a study conducted by Fan *et al*. in 2015, PbSe was doped with silver and antimony using a high-pressure method. The outcomes revealed that the co-doping with Ag and Sb resulted in a concurrent decrease in electrical resistivity and phonon thermal conductivity. This led to a notable improvement in thermoelectric performance, with the figure-of-merit increasing fivefold, reaching 1.03 at 600 K, in comparison to undoped PbSe. Peng *et al.* (2011) addressed the pressing need to understand the electronic structure and transport properties of doped PbSe for thermoelectric applications. They employed a first-principles approach to investigate the band structures of PbSe doped with various impurities, encompassing cation-site substitutional impurities like Na, K, Rb, Mg, Ca, Sr, Cu, Ag, Au, Zn, Cd, Hg, Ga, In, Tl, Ge, Sn, and anion-site substitutional impurities such as P, As, Sb, O, S, and Te. The study calculated the density of states (DOS) difference between the doped samples and the pure host sample. The results revealed a competition between electrical conductivity and Seebeck coefficient, indicative

The Role of Antimony in Tailoring Optical Properties of Spray Pyrolysis Synthesized PbSe/Sb Thin Films for Solar Device Optimization

296

of typical thermoelectric behavior. In their 2021 study, Chandekar *et al.* explored the structural, vibrational, optical, dielectric, and electrical properties of both undoped and Pr:PbS nanoparticles (NPs), identifying their suitability for optoelectronic devices. The analysis revealed crystallite sizes ranging from 14 to 18 nm, lattice strains between 1.6×10^{-4} and 2.2×10^{-4}, and dislocation densities ranging from 3.0×10^{-3} to 4.8×10^{-3} for the prepared NPs. The Optical band gap measurements indicated values of 1.414 eV for undoped NPs, and 1.494 eV, 1.402 eV, and 1.458 eV for NPs doped with 0.5 wt%, 1.0 wt%, and 2.5 wt% of Pr:PbS, respectively. Furthermore, the study derived ideality factors from the current-voltage characteristic, yielding values of 1.46, 1.42, 1.47, and 1.60 for undoped NPs and those doped with 0.5 wt%, 1.0 wt%, and 2.5 wt% of Pr:PbS, respectively. The findings present PbS a potential nanoparticles materials in optoelectronic device applications.

MATERIALS AND METHODS

In this study, lead selenide thin films, both doped with antimony and undoped, were produced through the spray pyrolysis technique at an elevated temperature of 200°C. The impact of antimony doping on PbSe was examined using a Unico UV-2102 Pc spectrophotometer, with light incidence at a normal angle, within the wavelength range of 320-1500nm.

Glass slides surfaces measuring 76mm x 25mm x 1mm were meticulously cleaned by immersing them in a concentrated HCl solution for two days to remove grease. Subsequently, they underwent thorough scrubbing with a cold detergent solution and a soft synthetic fiber sponge. The cleaned glass surfaces were then rinsed with distilled water and dried in an oven ensuring the production of adhesive and uniformly deposited films. Two (2) glass beakers (50 ml and 100 ml), two (2) stirring rod, three (3) clinical syringes (5 ml and 10 ml), four (4) measuring cylinders (50 ml and 100 ml), five (5) spatulas and six (6) clamps were cleaned with detergent solution, rinsed with distilled water and dried.

Two baths were prepared, one contained antimony and the other without antimony. The glass substrates were placed in the pyrolysis deposition chamber, and the solution from each bath was sprayed onto the substrates through the atomizer nozzle. The first bath included 5 ml of 1.69 g $PbCl_2$, 5 ml of 2.1 g Na_2SeSO_3, 10 ml of EDTA, 5ml of 1.76g Sb/Cl_2, and 25 ml of water, totaling 50 ml. The second bath mirrored the first but excluded antimony and contained 30 ml of distilled water instead of 25 ml. The spraying occurred at an elevated temperature in the pyrolysis chamber, and the sprayed substrates were left in the deposition chamber for 5 minutes at a temperature of 200°C. After deposition, some materials were directly characterized, while others were annealed before characterization.

RESULTS
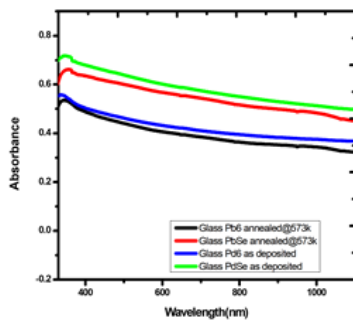
Figures 1: Plot of Absorbance Vs wavelength for PbSe & Pb₆ on glass
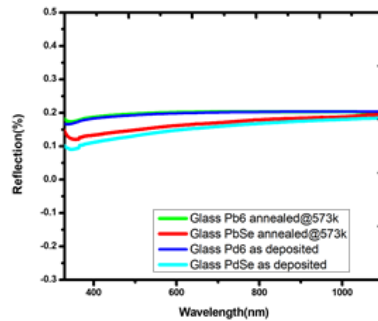
Figures 2: Plot of reflectance Vs wavelength for PbSe & Pb₆ on glass
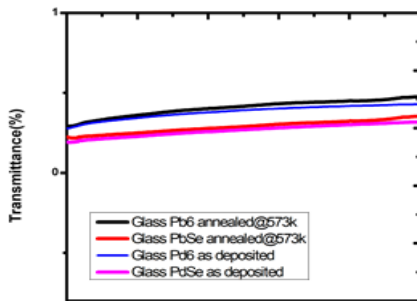
Figure 3: Plot of transmittance Vs wavelength for PbSe & Pb₆on glass
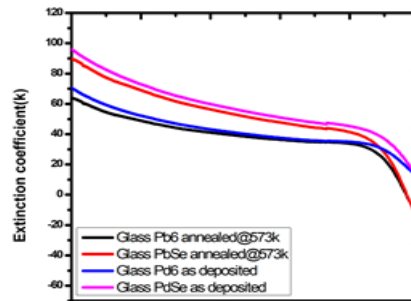
Figure 4: Plot of Extinction coefficient Vs wavelength for PbSe & Pb₆on glass

The Role of Antimony in Tailoring Optical Properties of Spray Pyrolysis Synthesized PbSe/Sb Thin Films for Solar Device Optimization

297
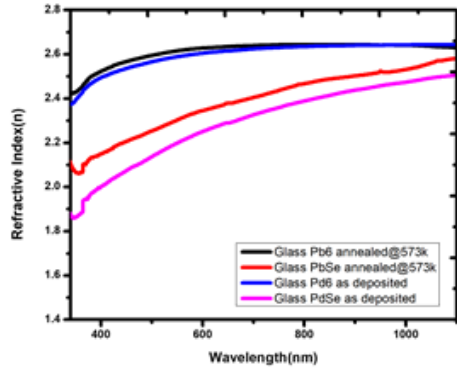
Figure 5: Plot of refractive index Vs wavelength for PbSe &Pb6
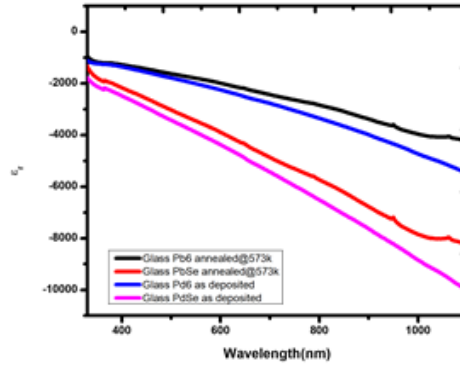
Figure 6: Plot of real dielectric constant Vs wavelength for PbSe &Pb6
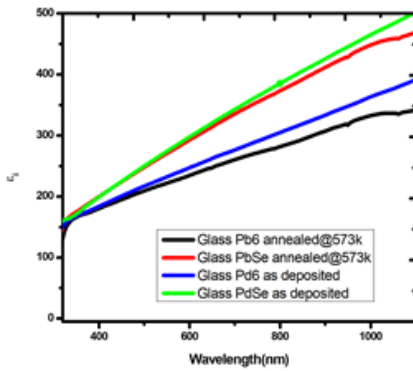
Figure 7: Plot of Imaginary dielectric constant Vs wavelength for PbSe & Pb6
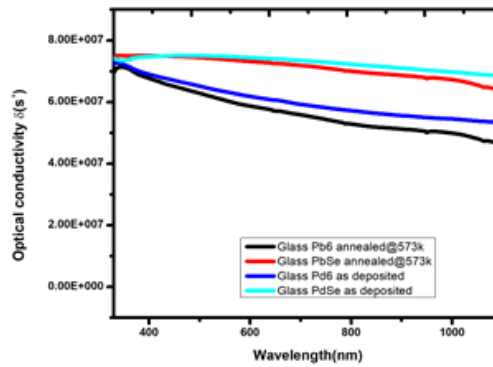
Figure 8: Plot of Optical conductivity Vs wavelength for PbSe & Pb6

Figure 9: A graph of $(\alpha h\upsilon^2)$ Vs hυ for PbSe & Pb6

The Role of Antimony in Tailoring Optical Properties of Spray Pyrolysis Synthesized PbSe/Sb Thin Films for Solar Device Optimization

298
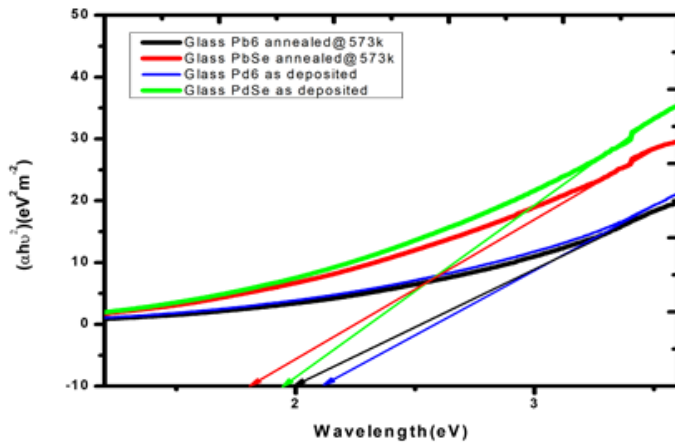
DISCUSSION

Figure 1 displays the absorbance plot against wavelength (λ) for both PbSe and Pb6 (PbSe/Sb). Initially, undoped PbSe exhibited a higher absorbance value of 0.70, which decreased to 0.60 upon annealing at 573K in the Near Ultraviolet (NUV) region. This reduction in absorbance extends gradually towards the Infrared (IR) region of the spectrum. The as-deposited sample of Antimony-doped PbSe displayed an absorbance of 0.55, which further decreased to 0.51 at a wavelength of 340 nm after annealing. Across all samples, absorbance consistently decreased towards the IR region of the spectrum. The notable high absorbance in the NUV region suggests potential applications for these thin films in thermal control window coatings, making them suitable for roofing in poultry buildings (Mphande & Pogrebnoi, 2014, Hernandez-Calderon, 2018).

Figure 2 presents the plot of reflectance against wavelength for undoped PbSe and doped PbSe (Pb$_6$), revealing an inverse characteristic compared to absorbance. Notably, both the as-deposited samples of antimony-doped and undoped PbSe exhibited lower reflectance than their respective annealed samples. This suggests that the introduction of antimony into PbSe does not impact the reflection of the films, and, interestingly, annealing serves to increase reflectance of the films.

A close look at Fig.3 indicates that the transmittance of the films exhibits an increasing trend with wavelength. Generally, these films demonstrate low transmittance in the Near Ultraviolet to Visible (NUV-VIS) range of the spectrum, with an upward trend towards the Infrared (IR) region. Remarkably, Antimony-doped lead selenide shows higher transmittance than undoped PbSe, although this value decreases upon annealing at 573K. This observation suggests that, for achieving higher transmittance, selecting Antimony-doped PbSe is preferable.

Figure 4 illustrates the relationship between the extinction coefficient and photon energy for both PbSe and PbSe/Sb. The extinction coefficient, which measures how strongly a substance absorbs light at a specific wavelength, decreases as photon energy increased. The undoped sample initially has the highest value of 95 at 1.25 eV, which decreases to 90 after annealing. Antimony-doped samples exhibit lower extinction coefficients, with values of 7.0 for the as-deposited and 65 for the annealed Pb$_6$ sample at the same energy level of 1.25 eV. Generally, the extinction coefficient decreases as photon energy increases. It was observed that doping PbSe with antimony reduces the extinction coefficient, and annealing also reduces absorbance. This is in line with (Kumar *et al.,* 2014, Ashraf *et al.,* 2016).

In Fig. 5, the refractive index is plotted against wavelength for both antimony-doped and undoped PbSe. The graph illustrates a notable increase in refractive index as the wavelength extends from 340nm to 1100nm. For undoped PbSe, the refractive index is 7.92, which rises to 8.43 at 1100nm after annealing at 573K. In contrast, antimony-doped PbSe exhibits a refractive index of 8.87, increasing to 9.07 in the infrared region following annealing at 573K. Notably, the doped sample shows a consistent trend with an overlap between 800 to 1000nm.

Figures 6 and 7 depict the real dielectric constant (ε_r) and imaginary dielectric constants (ε_I) plotted against the wavelength for both antimony-doped and undoped PbSe films. The two graphs exhibit an inverse relationship. Specifically, antimony-doped and annealed PbSe (Pb$_6$) demonstrates the highest ε_r value, while the undoped and un-annealed PbSe exhibits the lowest value, as highlighted in Figure 6.

Figures 8 and 9 illustrate the optical conductivity and band gaps of antimony-doped and undoped PbSe. In Figure 8, the undoped PbSe exhibits the highest optical conductivity, reaching 80.4 Mmho's at λ = 340nm, with the annealed undoped PbSe closely following. The undoped PbSe shows nearly uniform conductivity across the entire spectrum. Conversely, the antimony-doped PbSe (Pb6) displays lower optical conductivity, decreasing towards the infrared (IR) regions. It is observed that doping with Antimony results in reduced optical conductivity, and the annealing process similarly diminishes conductivity, this is in agreement with (Jena *et al.,* 2023, Leem & Yu, (2011), Nasser *et al.,* 2019).

The square absorption coefficient versus photon energy graphs for thin films of both Antimony-doped and undoped PbSe exhibit typical band gap curves. The optical band gap values were determined by analyzing the fundamental absorption, corresponding to electron excitation from the valence band to the conduction band and is as displayed in figure 9. In the as-deposited state, the Pb$_6$ (PbSe/Sb) sample displayed the largest band gap at 2.2 eV. However, annealing the sample at 573 K resulted in a reduction of the band gap to 2.0 eV. Similarly, the undoped PbSe sample initially had a band gap of 1.96 eV, which also decreased to 1.80 eV upon annealing at 573 K. This indicates that the process of doping PbSe with Antimony and annealing the films leads to a reduction in their band gaps.

Conclusion

Using the spray pyrolysis technique in an elevated temperature chamber, we successfully synthesized both Antimony-doped and undoped thin films of lead selenide. Spectrophotometric analysis revealed notable reduction in band gap values through Antimony doping and that annealing holds significant implications for tailoring the optical properties of PbSe films, particularly in the Near Ultraviolet (NUV) to Infrared (IR) range. The observed inverse relationship between reflectance and absorbance suggests that the introduction of Antimony does not significantly impact reflectance, while annealing enhances it, offering avenues for optimization in optoelectronic devices. The increasing trend in transmittance in the IR region for Antimony-doped PbSe indicates its potential for achieving higher transparency compared to undoped PbSe, although careful consideration is required during optimization. These enhancements position PbSe/Sb as a promising material for applications such as solar cell fabrication and anti-reflection coatings, particularly beneficial in cold climate regions. Given these distinctive characteristics, it can be concluded that Antimony-doped PbSe thin films are excellent candidates for thermal control window coatings, especially effective in cold climates.

Acknowledgements

REFERENCES

Akbari-Moghanjoughi, M. (2021). Energy band structure of multistream quantum electron system. Scientific Reports, 11(1), 21099. https://www.nature.com/articles/s41598-021-00534-w

Ashraf, M. T., Salah, N. A., Rafat, M., Zulfequar, M., & Khan, Z. H. (2016). Optical studies on Zn-doped lead chalcogenide (PbSe) 100− xZnx thin films composed of

The Role of Antimony in Tailoring Optical Properties of Spray Pyrolysis Synthesized PbSe/Sb Thin Films for Solar Device Optimization

299

nanoparticles. Thin Solid Films, 612, 109-115. https://doi.org/10.1016/j.tsf.2016.05.054

Ashraf, M. T., Salah, N. A., Rafat, M., Zulfequar, M., & Khan, Z. H. (2016). Optical studies on Zn-doped lead chalcogenide (PbSe) 100− xZnx thin films composed of nanoparticles. Thin Solid Films, 612, 109-115. https://doi.org/10.1016/j.tsf.2016.05.054

Ashraf, M. T., Salah, N., Rafat, M., & Khana, Z. H. (2017). Synthesis and characterization of indium doped lead chalcogenides (PbSe) 100− xInx thin films composed of QDs. Journal of Alloys and Compounds, 701, 850-857. https://doi.org/10.1016/j.jallcom.2017.01.193

Bera, R., Choi, D., Jung, Y. S., Song, H., & Jeong, K. S. (2022). Intraband transitions of nanocrystals transforming from lead selenide to self-doped silver selenide quantum dots by cation exchange. The Journal of Physical Chemistry Letters, 13(26), 6138-6146. https://doi.org/10.1021/acs.jpclett.2c01179

Chandekar, K. V., Shkir, M., Palanivel, B., Ahmad, Z., Algarni, H., & AlFaify, S. (2021). Comparative study of Pr-doped and undoped PbS nanostructures facilely synthesized for optoelectronic applications. Solid State Sciences, 122, 106773. https://doi.org/10.1016/j.solidstatesciences.2021.106773

Elsheikh, A. H., Sharshir, S. W., Ali, M. K. A., Shaibo, J., Edreis, E. M., Abdelhamid, T.,& Haiou, Z. (2019). Thin film technology for solar steam generation: A new dawn. Solar Energy, 177, 561-575. https://doi.org/10.1016/j.solener.2018.11.058

Endres, J., Egger, D. A., Kulbak, M., Kerner, R. A., Zhao, L., Silver, S. H., ... & Kahn, A. (2016). Valence and conduction band densities of states of metal halide perovskites: a combined experimental–theoretical study. The journal of physical chemistry letters, 7(14), 2722-2729. https://doi.org/10.1021/acs.jpclett.6b00946

Eslamian, M. (2017). Inorganic and organic solution-processed thin film devices. Nano-micro letters, 9(1), 3. https://link.springer.com/article/10.1007/s40820-016-0106-4

Fan, H., Su, T., Li, H., Du, B., Liu, B., Sun, H., ... & Jia, X. (2015). Enhanced thermoelectric performance of PbSe co-doped with Ag and Sb. Journal of Alloys and Compounds, 639, 106-110. https://doi.org/10.1016/j.jallcom.2015.03.117

Gayner, C., Sharma, R., Mallik, I., Das, M. K., & Kar, K. K. (2016). Exploring the doping effects of copper on thermoelectric properties of lead selenide. Journal of Physics D: Applied Physics, 49(28), 285104 DOI 10.1088/0022-3727/49/28/285104

Hernandez-Calderon, I. (2018). Optical properties and electronic structure of wide band gap II-VI semiconductors. In II-VI semiconductor materials and their applications (pp. 113-170). Routledge.

Jena, B. J., Alagarasan, D., Kumar, J., & Naik, R. (2023). Phase change, tuning of optical and dielectric parameters in Bi/S-Se-Sb heterostructure film upon thermal annealing: An experimental and computational approach. Journal of Alloys and Compounds, 968, 171873. https://doi.org/10.1016/j.jallcom.2023.171873

Kumar, R., Das, R., Gupta, M., & Ganesan, V. (2014). Preparation of nanocrystalline Sb doped PbS thin films and their structural, optical, and electrical characterization. Superlattices and microstructures, 75, 601-612. https://doi.org/10.1016/j.spmi.2014.08.019

Leem, J. W., & Yu, J. S. (2011). Physical properties of electrically conductive Sb-doped SnO2 transparent electrodes by thermal annealing dependent structural changes for photovoltaic applications. Materials Science and Engineering: B, 176(15), 1207-1212. https://doi.org/10.1016/j.mseb.2011.06.015

Lewis, N. S. (2016). Research opportunities to advance solar energy utilization. Science, 351(6271), aad1920. https://doi.org/10.1126/science.aad1920

Lifshitz, E., Brumer, M., Kigel, A., Sashchiuk, A., Bashouti, M., Sirota, M., & Zyss, J. (2006). Air-Stable PbSe/PbS and PbSe/PbSe x S1-x Core− Shell Nanocrystal Quantum Dots and Their Applications. The Journal of physical chemistry B, 110(50), 25356-25365. https://doi.org/10.1021/jp0644356

Mphande, B. C., & Pogrebnoi, A. (2014). Impact of extraction methods upon light absorbance of natural organic dyes for dye sensitized solar cells application. Journal of Energy and Natural Resources, 3(3), 38-45. 10.11648.j.jenr.20140303.13-libre.pdf

Nasser, R., Othmen, W. B. H., & Elhouichet, H. (2019). Effect of Sb doping on the electrical and dielectric properties of ZnO nanocrystals. Ceramics International, 45(6), 8000-8007. https://doi.org/10.1016/j.ceramint.2018.12.089

Nelson, R. (2000). Intel's site selection decision in Latin America. Thunderbird International Business Review, 42(2), 227.Intels-site-selection-decision-in-Latin-America.pdf

Nishikawa, M., Shiroishi, W., Honghao, H., Suizu, H., Nagai, H., & Saito, N. (2017). Probability of Two-Step Photoexcitation of Electron from Valence Band to Conduction Band through Doping Level in TiO2. The Journal of Physical Chemistry A, 121(32), 5991-5997. https://doi.org/10.1021/acs.jpca.7b05214

Nworie Ikechukwu C., Agbo P.E, Oko K. I., Brown N. W. & Ugah J. O. (2023). "Energy And Economic Evaluation Of The 3000kwp Grid Connected Photovoltaic Power Plant In Umuoghara Quarry Industrial Cluster, Nigeria". *Journal of the Nigerian Association of Mathematical Physics Volume 65, (October 2022 – August 2023 Issue), pp21 – 26 © J. of NAM* https://nampjournals.org.ng/index.php/home/article/view/4

Peng, H., Song, J. H., Kanatzidis, M. G., & Freeman, A. J. (2011). Electronic structure and transport properties of doped PbSe. Physical Review B, 84(12), 125207. DOI:https://doi.org/10.1103/PhysRevB.84.125207

Saunders, E. L. (2020). Chipping away at globalisation: transnational labour organising in the semiconductor industry. https://era.ed.ac.uk/handle/1842/37295

Xia, M., Yan, X., Li, H., Wells, N., & Yang, G. (2020). Well-designed efficient charge separation in 2D/2D N doped La2Ti2O7/ZnIn2S4 heterojunction through band structure/morphology regulation synergistic effect. Nano Energy, 78, 105401. https://doi.org/10.1016/j.nanoen.2020.105401

Zhang, Q., Cao, F., Lukas, K., Liu, W., Esfarjani, K., Opeil, C., & Ren, Z. (2012). Study of the thermoelectric properties of lead selenide doped with boron, gallium, indium, or thallium. Journal of the American Chemical Society, 134(42), 17731-17738. https://doi.org/10.1021/ja307910u

The Role of Antimony in Tailoring Optical Properties of Spray Pyrolysis Synthesized PbSe/Sb Thin Films for Solar Device Optimization

300